



## Computational catalysis

Computational study of  $P^tBu_3$  as ligand in the palladium-catalysed amination of phenylbromide with morpholine<sup>☆</sup>Claire L. McMullin, Bastian Rühle<sup>1</sup>, Maria Besora<sup>2</sup>, A. Guy Orpen, Jeremy N. Harvey\*, Natalie Fey\*\*

School of Chemistry, University of Bristol, Cantock's Close, Bristol BS8 1TS, UK

## ARTICLE INFO

Article history:  
Available online 3 March 2010

Keywords:  
Computational  
Palladium catalysis  
C–N coupling  
Ligand effects

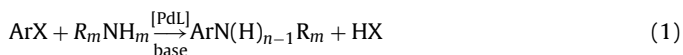
## ABSTRACT

We have investigated the full catalytic cycle for the coupling of phenylbromide with morpholine (Buchwald–Hartwig amination), catalysed by the synthetically relevant  $Pd(P^tBu_3)$  complex, with computational methods. The experimentally observed utility of this catalyst can be related to the energetically accessible ligand dissociation from the initial  $Pd(0)$  species, combined with a low barrier to oxidative addition and sterically unfavourable dimer formation. Furthermore, the steric bulk of the  $P^tBu_3$  ligand allows for a low-coordinate, dissociative pathway and facile reductive elimination over the competing, undesirable  $\beta$ -hydride elimination pathway. Evaluating the full catalytic cycle with one of the most versatile catalyst complexes used experimentally has allowed us to evaluate the most likely catalytic pathway and relate this to general ligand design criteria, as well as providing validation for the computational approach used.

© 2010 Elsevier B.V. All rights reserved.

## 1. Introduction

Over the last decade, palladium-catalysed C–N cross-coupling reactions (Eq. (1)), often named Buchwald–Hartwig aminations after two of the main contributors to the field, have found widespread use in synthetic chemistry (see Refs. [1–8] for recent reviews), including in an industrial, large-scale production setting [5,7,8].



Apart from the utility of forming aromatic C–N bonds for a wide range of substrates, a key factor in making this class of reactions synthetically useful is that their activity for a given substrate can often be optimised by modifying the ligand(s) attached to the transition metal centre [1,3,6–12]. The resulting versatility of the family of cross-coupling reactions has been instrumental in the search for active catalysts, e.g. for arylchloride substrates, which are usually cheaper, but less reactive than the corresponding arylbromides [6,11,13–15].

Significant gains can often be achieved by careful optimisation of both the catalytically active species and the reaction conditions, yet few general and reliable catalysts are available. In general, good results can be achieved with bulky, electron-rich ligands and the set of successful ligands (Fig. 1) includes e.g.  $P^tBu_3$  **I** [16–18], Buchwald's class of biaryl ligands **II** [3], Verkade's bicyclic triaminophosphine ligand **III** [19], Beller's adamantyl substituted CatacXium A **IV** [20,21], several chelating ligands such as BINAP **V** [22], DPPF **VI** [12,23], and Josiphos **VII** [11], as well as N-heterocyclic carbenes of general structure **VIII** [24]; many of these ligands have been patented [7,8]. The success of the subset of bulky, electron-rich monodentate ligands has generally been suggested to be related to the stabilisation of low-coordinate palladium complexes by secondary interactions [18,25–27], facilitating catalyst initiation/oxidative addition. Ligand bulk has also been implicated in making an undesirable  $\beta$ -hydride elimination pathway less favourable relative to reductive elimination [27–31].

The discovery and optimisation of novel ligand types active in cross-coupling reactions and, more specifically, in palladium-catalysed aminations, currently attracts considerable research interest (see reviews cited above), and the high-throughput screening of ligands can yield useful results [32]. In parallel with such searches, research has also focussed on establishing the detailed mechanism of amination and related cross-coupling reactions, as well as the impact of modifying key reaction variables. Experimental mechanistic investigations (see e.g. Refs. [12,15,17,22,30,33–36]) have been supplemented by computational studies of the reaction mechanism (for recent examples, see Refs. [13,25–27,31,37–48]) covering key steps or indeed the full

<sup>☆</sup> This paper is part of a special issue on Computational Catalysis.

\* Corresponding author. Tel.: +44 117 9546991; fax: +44 117 9251295.

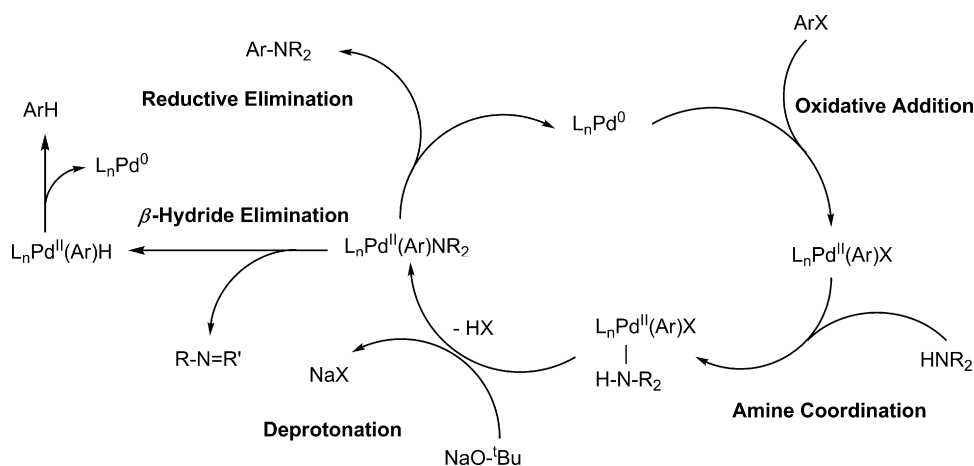
\*\* Corresponding author. Tel.: +44 117 3318260; fax: +44 117 9251295.

E-mail addresses: [Jeremy.Harvey@Bristol.ac.uk](mailto:Jeremy.Harvey@Bristol.ac.uk) (J.N. Harvey),

[Natalie.Fey@Bristol.ac.uk](mailto:Natalie.Fey@Bristol.ac.uk) (N. Fey).

<sup>1</sup> Present address: Ludwig-Maximilians Universität, München, Germany.

<sup>2</sup> Present address: ICIQ (Institut Català d'Investigació Química), Tarragona, Spain.



**Scheme 1.** General reaction mechanism for palladium-catalysed C–N coupling.

catalytic cycle of cross-coupling reactions, including aminations [25,26,44,45].

Traditionally, such modelling studies of C–N coupling have had to rely on small model complexes [37,38,45] or layered approaches (ONIOM, QM/MM [49]) [31,50], which were unable to capture the steric and electronic properties of the catalytically active species fully. However, only computational studies of the systems used experimentally allow us to compare experimental and computational observations with confidence, thus both validating the computational approach and providing useful insights into the experimental data. Recent technological developments have made such computational studies of the catalytic cycle accessible [9,25,26], although conformational flexibility, isomerism and multiple reaction pathways remain significant challenges in the computational study of synthetically relevant complexes.

As part of an ongoing large-scale exploration of ligand effects in transition metal complexes [51], we are interested in probing the mechanistic consequences of changing the ligand on a range of reactions. Fundamental to such work is a fully mapped catalytic cycle and here we describe our exploration of a likely catalytic cycle (Scheme 1), exploring ligand effects on the potentially competing elimination pathways, as well as possible side-reactions and dimeric reservoir species. We have focussed here on palladium complexes with  $P^tBu_3$ , **I**, as this ligand is widely used but conformationally rigid, allowing us to confirm the most likely reaction mechanism without having to consider complications arising from conformational responsiveness [9,25,26]. Morpholine, our chosen substrate, is also reasonably rigid, provides a  $\beta$ -hydrogen, thus allowing evaluation of the competing elimination pathways, and has been used synthetically as a substrate for ligand screening, see e.g. [19,52].

## 2. Computational details

Geometries were initially optimised in the gas phase using the popular B3LYP density functional [53,54] as implemented in Jaguar [55], with the 6–31G basis set on all atoms except for Pd and Br, where the effective core potential basis set LACVP as implemented in Jaguar was used (labelled as BS1). Test calculations on selected intermediates and transition states involved in the oxidative addition show that adding polarisation functions on the non-H atoms leads to small changes in bond lengths and angles upon re-optimization, but without any significant effect on relative energies. All stationary points were verified by calculation of vibrational frequencies and for transition states the nature of the calculated eigenvector corresponding to the imag-

**Table 1**

Single point ligand dissociation energies (in kcal mol<sup>-1</sup>, in the gas phase) for  $PH_3$  from  $Pd(PH_3)_2$ . All geometries optimised with B3LYP/BS1.

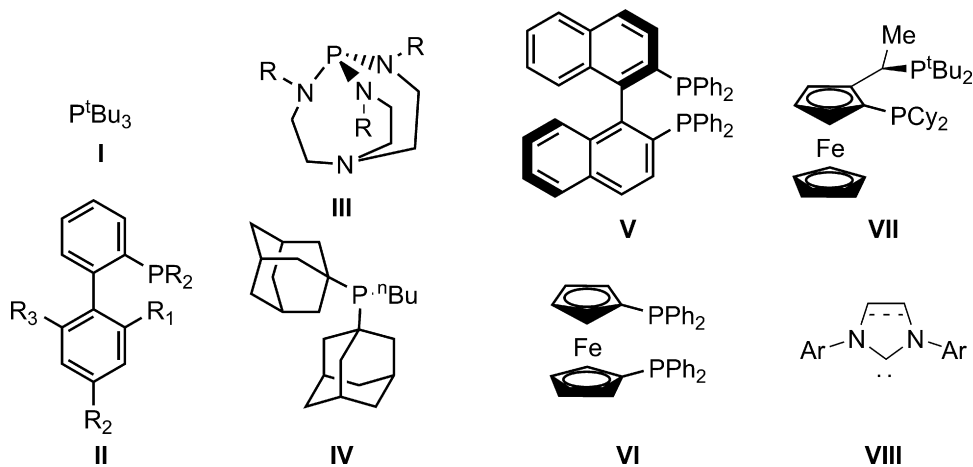
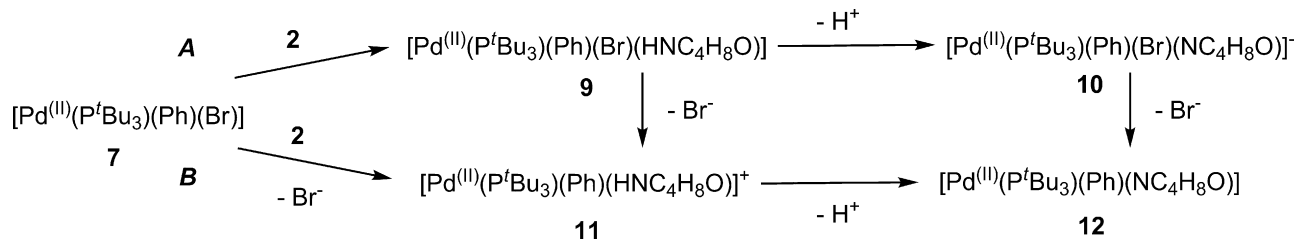
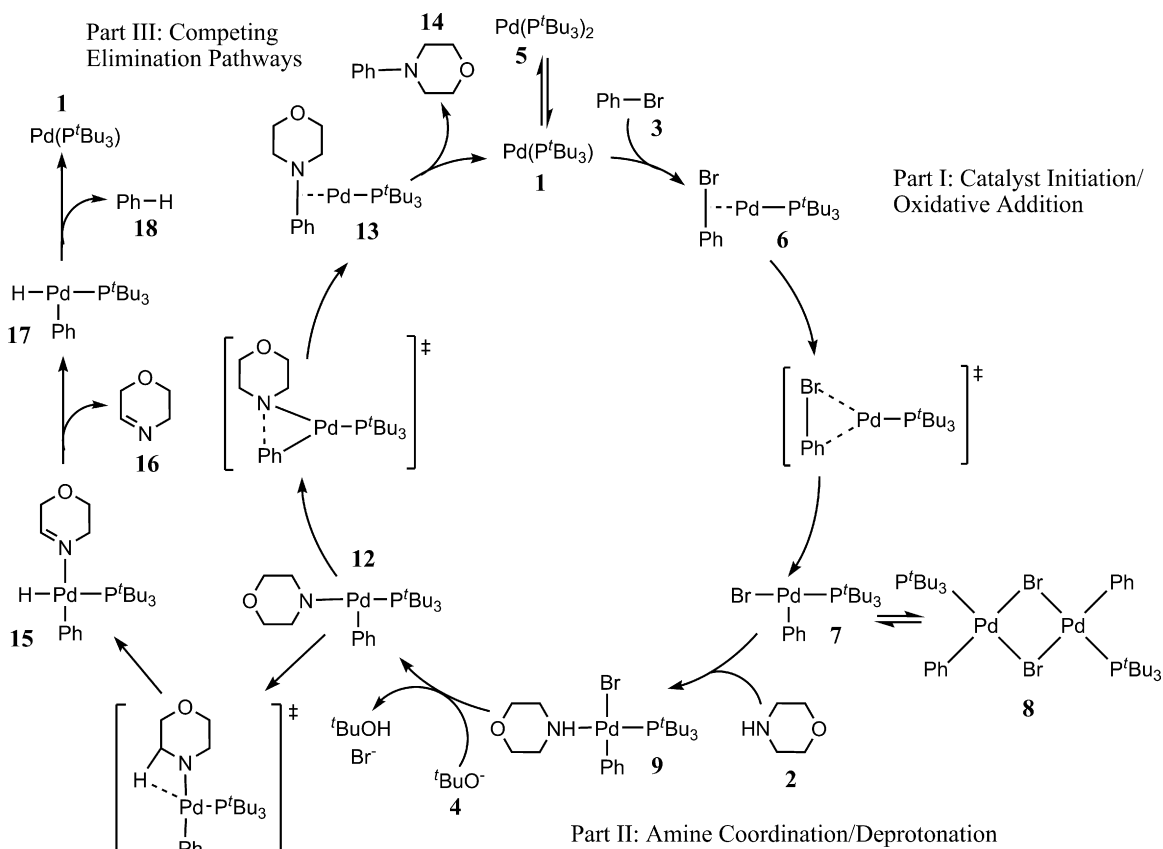
Method/basis set and basis set for ECP atoms	Energy (kcal mol <sup>-1</sup> )
B3LYP/BS1	25.78
B3LYP/BS2	28.43
BP86/BS2	33.01
SCS-MP2/BS3	30.25
MP2/BS3	35.85
CCSD(T)/BS3	32.12
CCSD(T)/BS4	31.57

inary frequency was checked to be consistent with the expected transformation. Gas phase single point energies were calculated for these B3LYP/BS1 geometries using a larger basis set combination (BS2), with Jaguar's effective core potential basis set LACV3P for Pd and Br, and 6–311+G\*\* on all other atoms. The B3LYP/BS2 energies were calculated with ultrafine DFT grids and tight cutoffs for SCF convergence.<sup>3</sup>

To identify the most suitable computational approach, the ligand dissociation energy from  $PdL_2$  was calculated for  $L = PH_3$  using Møller–Plesset second-order perturbation theory (MP2), two different density functional theories (B3LYP and BP86), and coupled cluster methods; these results are summarised in Table 1. These used B3LYP/BS1 optimised geometries throughout, BS2 as detailed above, and the BP86 functional [53,56] as implemented in Jaguar [55]. Single point energies with Møller–Plesset second-order perturbation theory (MP2) [57] and coupled cluster calculations with both single and double substitutions and non-iterative triple excitations (CCSD(T)) [58] were calculated in Gaussian [59], using the standard 6–31+G\*\* basis set on all atoms except for Pd and Br, where the Stuttgart/Dresden effective core potential [60] and the associated basis sets as implemented in Gaussian were used (BS3). Molpro [61] was used to calculate single point energies with the CCSD(T) approach [62] using an expanded basis set (BS4) including the Stuttgart/Dresden effective core potential on Pd [60] with an associated (8s7p6d2f1g)/[6s5p3d2f1g] valence basis set [63], and the cc-pVTZ basis [64] on other elements. The scaling parameters used to calculate spin-component scaled MP2 energies (SCS-MP2) were 1/3 for parallel-spin pair correlation energy and 6/5 for antiparallel-spin pair correlation energy [65].

Given the size of the complexes investigated in this work, only the DFT approaches are feasible for a detailed exploration of the catalytic cycle. At this level of theory, the most pronounced

<sup>3</sup> Additional keywords: gdfitfine=-13, gdfitmed=-13, gdfitgrad=-13, iacc=1.



improvement of ligand dissociation energies can be achieved by increasing the size of the basis set. The B3LYP/BS2 dissociation energies are lower than the more accurate CCSD(T) and SCS-MP2 values, whereas the BP86/BS2 energies are slightly higher. The B3LYP density functional was also used by Cundari and Deng [45], and they found results comparable to the CCSD(T) level of theory for the SBK(d) basis set. The general conclusion from this limited ab initio benchmark study with large basis sets BS3 and BS4 is that the error in the B3LYP/BS2 results is acceptably small given the mainly qualitative purposes of this work. Nevertheless, some of the calculated energetics are clearly far from quantitative at the B3LYP level as the functional is unable to capture dispersion interactions fully (see e.g. Ref. [66] for a recent discussion), thus favouring ligand dissociation as observed here, and this is significant when attempting detailed comparison with experiment.

Unless stated otherwise, the results reported in the remainder of this manuscript have been calculated using B3LYP/BS1 for geometry optimisations and frequency calculations, needed to derive zero-point energy (ZPE) corrections, and we report energy differences  $\Delta E$  calculated from single point  $E_{\text{B3LYP/BS2}} + \text{ZPE}_{\text{B3LYP/BS1}}$  energies throughout. We have also explored the energies of key species with the SCS-MP2/BS3 approach and these energies have been included in the Supporting Information.

For Section 3.2, solution phase single point energies have been calculated with B3LYP/BS2, using the Poisson Boltzmann polarised continuum solvation model [67] as implemented in Jaguar with toluene ( $\epsilon = 2.379$ , probe radius = 2.757) as the solvent. These energies have been corrected with gas phase B3LYP/BS1 ZPE estimates. Senn and Ziegler identified stepwise halide dissociation followed by Pd–C bond formation as an energetically feasible pathway for the oxidative addition when solvation effects were taken into account during geometry optimisation, but were unable to confirm the concerted mechanism identified in the gas phase [68]; this observation has been supported by Norrby et al. [69]. However, for the large complexes considered here we found geometry convergence slow and unreliable when including solvation, and have thus only considered single point solvated energies where charged species are involved.

### 3. Results and discussion

The catalytic cycle considered here is shown in Scheme 2, which also illustrates the numbering system used throughout this work; alternative pathways considered for the amine coordination/deprotonation step are shown in Scheme 3. The discussion is divided into three main headings: catalyst initiation/oxidative addition (Section 3.1), amine coordination/deprotonation (Section 3.2) and elimination pathways (Section 3.3).

#### 3.1. Catalyst initiation/oxidative addition

The oxidative addition of aryl halides to Pd(0) complexes is the first step in many palladium-catalysed reactions and may be rate determining in some cases [17,22]. The necessary increase in the metal oxidation state can be facilitated by electron-rich spectator ligands, a feature shared by most of the ligands shown in Fig. 1 [7]. Much recent computational work has thus covered this initial step, seeking to establish likely catalytic cycles for a range of cross-coupling reactions [25,37,41,44–46], to explore different factors such as solvent [13,44,68], substrate [13,42,68] and ligand effects [42,43,70], and to assess the possible role of anionic species [38,40]. However, with the exception of Buchwald's recent work [25], computational studies of amination have used model complexes, hampering comparison with experimental data. In this work we have assumed the catalytic cycle starts from Pd( $\text{P}^t\text{Bu}_3$ )<sub>2</sub>, **5**,

and proceeds via a neutral, dissociative pathway; this assumption is supported *inter alia* by calculations by Shaik and co-workers suggesting that the anionic pathway is less likely for electron-donating ligands and bromide counterions [71]. It is worth noting that this initial step could also proceed via oxidative addition of phenylbromide to a range of [Pd( $\text{P}^t\text{Bu}_3$ )X] complexes, where X could be ligand **1** [34,36], solvent [44], counterion [38,40] or amine substrate, followed by dissociation of X to form **7**, or reaching the coordinatively saturated complex **9** by a different route altogether.

This uncertainty about the exact mechanistic pathway leading to the product of oxidative addition **7** leads to difficulties when seeking to compare computational results with experiment. In particular, it is not obvious that it is appropriate to compare the calculated ligand dissociation energy (or free energy) from **5** with the experimental activation energy or free energy. Ligand dissociation from **5** may be a complicated process, with the formal product of ligand loss, monoligated Pd( $\text{P}^t\text{Bu}_3$ ) **1**, being able to interact with solvent molecules or other species present in the reaction mixture to stabilise the low-coordinate metal centre (see e.g. Refs. [37,42,44,68] for a more detailed discussion). Indeed, there is still further complication due to the existence of yet another mechanistic possibility [72], whereby monoligated Pd( $\text{P}^t\text{Bu}_3$ ) is never formed as an isolated species, but instead concerted substitution occurs from Pd( $\text{P}^t\text{Bu}_3$ )<sub>2</sub> to yield species such as Pd( $\text{P}^t\text{Bu}_3$ )(ArX). In the present contribution, whose focus is not on the details of the catalyst activation and oxidative addition steps, we do not explore all these possible variations in detail, and simply assume that the mechanism shown in Scheme 2 is correct.

Irrespective of these aspects, it is important to use a computational method that describes the Pd–L ligand bond energy accurately. As indicated in the computational details section, we have explored method performance for dissociation of a model ligand from PdL<sub>2</sub> and our chosen DFT approach gives reasonable agreement with higher levels of theory. The calculated ligand dissociation energy (we report energies as  $\Delta E = \Delta E_{\text{B3LYP/BS2}} + \Delta \text{ZPE}_{\text{B3LYP/BS1}}$  unless stated otherwise) for Pd( $\text{P}^t\text{Bu}_3$ )<sub>2</sub> is quite high at 29.7 kcal mol<sup>-1</sup>, but this step is entropically favourable and hence has a more favourable free energy ( $\Delta G = 17.7$  kcal mol<sup>-1</sup> at B3LYP/BS1 level) which should be feasible, especially at elevated reaction temperatures. This is also in agreement with a recent computational study of the same step considered as part of the Stille reaction, reporting  $\Delta E = 30.5$  kcal mol<sup>-1</sup> and  $\Delta G = 17.4$  kcal mol<sup>-1</sup> for the dissociation of one  $\text{P}^t\text{Bu}_3$  from Pd( $\text{P}^t\text{Bu}_3$ )<sub>2</sub> [46].

For the bulky  $\text{P}^t\text{Bu}_3$  ligand, the most likely catalytic pathway will involve monophosphine intermediates, suggesting that the oxidative addition of ArX will proceed via a dissociative mechanism [37,42,46]. Indeed the product of oxidative addition **7** has been characterised crystallographically [27], showing only a single  $\text{P}^t\text{Bu}_3$  ligand, and the most active catalysts are generated in situ from a 1:1 ratio of ligand to palladium derived from different precursors [73]. Recent experimental studies have hinted at a more complicated catalyst initiation pathway [34–36,74], but this lies outside the scope of the present work.

Prior to oxidative addition, the phenyl bromide **3** can coordinate to the metal centre via the aromatic ring or the halide atom. In line with previous work [41,45,68], isomers for the possible  $\pi$  interactions with the ring are quite similar in energy, with an  $\eta^2$ -interaction with the meta and para C atoms of the ring lowest in energy, whereas a complex bound via the halide [75] lies noticeably higher in energy. This coordination of the PhBr substrate occupies the vacant coordination site in a linear complex with **6** lying 15.0 kcal mol<sup>-1</sup> lower in energy than **1**. The lowest barrier to oxidative addition in the gas phase for the monoligated complex **6** [Pd<sup>0</sup>( $\text{P}^t\text{Bu}_3$ )(PhBr)] is 3.3 kcal mol<sup>-1</sup> and the reaction product **7** [Pd<sup>II</sup>( $\text{P}^t\text{Bu}_3$ )(Ph)(Br)] lies lower in energy than **6** by 14.0 kcal mol<sup>-1</sup>.

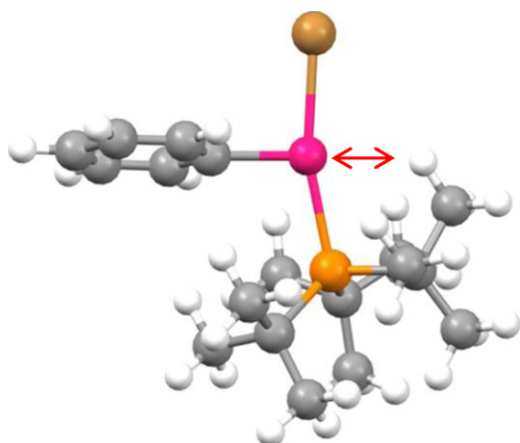


**Fig. 2.** Agostic interaction observed in structure **7** between a C–H bond of the ligand **I** and the palladium(II) metal centre.

There are three possible T-shaped isomers of **7** from this reaction step, and the energetically most favourable isomer has the phosphine ligand *trans* to the bromide, in line with expected *trans* influences, placing the strongest donor ( $\text{Ph}^-$ ) *trans* to the vacant site (see also Ref. [45]). The energies of other isomers of **7** are included in the Supporting Information.

In agreement with the crystallographically observed geometry [27], an interesting  $\gamma$ -agostic interaction is observed for **7**, with a hydrogen in reasonably close proximity to the palladium(II) metal centre ( $\text{H} \cdots \text{Pd}$  of 2.51 Å, cf. 2.18 Å from idealised positions in the crystal structure geometry [27]), as shown in Fig. 2, essentially protecting the vacant coordination site with steric bulk. Similar interactions have been identified for the ligands considered by Buchwald and Barder [25], and the importance of these interactions in stabilising low-coordinate palladium complexes has been explored computationally [70].

Dimerisation of the low-coordinate complex **7** of this oxidative addition step would also serve to occupy the fourth coordination site on the square-planar palladium. Such halide-bridged dimers have been observed crystallographically for slightly less hindered ligands, such as S-Phos (**II** with  $\text{R} = \text{Cy}$ ,  $\text{R}_1, \text{R}_3 = \text{OMe}$  and  $\text{R}_2 = \text{H}$ ) [76], CataCXium A, **IV** [20], and  $\text{P}(o\text{-tolyl})_3$  [77] as well as for a chloride complex of  $\text{P}^t\text{Bu}_3$  **I** [34]; in this last example the authors have confirmed predominantly monomeric species in solution. We have been unable to perform the frequency calculations necessary to obtain ZPE corrections in this case, but without these the resulting complex  $[\text{Pd}_2(\mu\text{-Br})_2(\text{P}^t\text{Bu}_3)_2(\text{Ph})_2]$  **8** lies 6.7 kcal mol $^{-1}$  lower in energy than two monomers **7**. The dimer **8** would be entropically disfavoured, reducing this energy difference further. On the other hand, consideration of dispersion effects would likely make this complex more favourable due to attractive interactions between the ligands and Ph rings. Here we conclude that while this complex may act as a reservoir species lying off the catalytic cycle, this dimer is not a deep minimum on the potential energy surface for bulky ligands such as  $\text{P}^t\text{Bu}_3$  **I**; this may contribute to the catalytic utility of such ligands. A recent computational study by Lledós et al. has explored ligand effects on dimerisation, solvent coordination and the stability of monomeric species further [70] and reported Gibbs free energies both in the gas phase and with solvation which favour the monomeric complex **7**.

### 3.2. Amine coordination and deprotonation

The amine, in our chosen model morpholine, **2**, which is generally present in excess for this catalytic cycle, could also be coordinated in the vacant site of complex **7** (Scheme 3, route A);

**Table 2**

Energies for amine coordination and deprotonation steps, see Scheme 3 for complex numbering (relative energies calculated with solvation model,  $\Delta E_{\text{solv}} = \Delta E_{\text{B3LYP/BS2,solv}} + \Delta ZPE_{\text{B3LYP/BS1}}$ ); L *trans* to amine.

Intermediate		$\Delta E_{\text{solv}}$ (kcal mol $^{-1}$ )
<i>Pathway A</i>		
$[\text{Pd}^{\text{II}}(\text{P}^t\text{Bu}_3)(\text{Ph})(\text{Br})] + \text{HNC}_4\text{H}_8\text{O}$	<b>7</b>	0.00
$[\text{Pd}^{\text{II}}(\text{P}^t\text{Bu}_3)(\text{Ph})(\text{Br})(\text{HNC}_4\text{H}_8\text{O})]$	<b>9</b>	−7.75
$[\text{Pd}^{\text{II}}(\text{P}^t\text{Bu}_3)(\text{Ph})(\text{Br})(\text{NC}_4\text{H}_8\text{O})]^- + \text{H}^{\text{+a}}$	<b>10</b>	−4.60
$[\text{Pd}^{\text{II}}(\text{P}^t\text{Bu}_3)(\text{Ph})(\text{NC}_4\text{H}_8\text{O})] + \text{H}^{\text{+a}} + \text{Br}^-$	<b>12</b>	−11.58
<i>Pathway B</i>		
$[\text{Pd}^{\text{II}}(\text{P}^t\text{Bu}_3)(\text{Ph})(\text{HNC}_4\text{H}_8\text{O})]^{\text{+}} + \text{Br}^-$	<b>11</b>	40.20

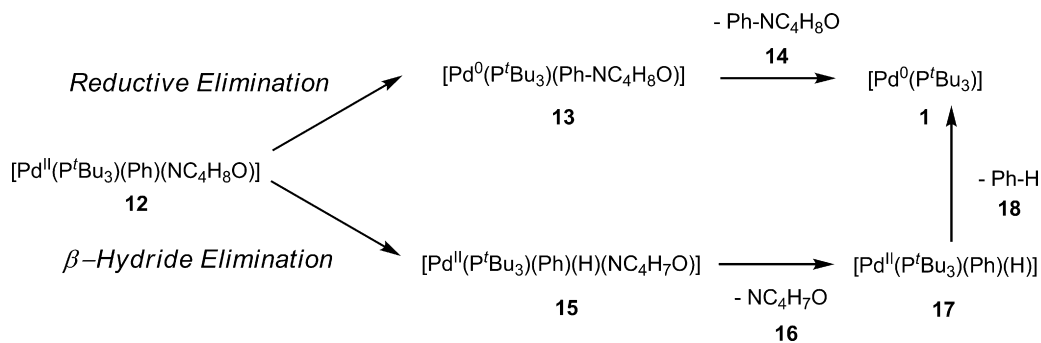
<sup>a</sup> Modelled as  ${}^t\text{BuOH}$ .

this would lock the palladium complex in the productive pathway and has indeed been observed crystallographically for the S-Phos ligand (**II** with  $\text{R} = \text{Cy}$ ,  $\text{R}_1, \text{R}_3 = \text{OMe}$  and  $\text{R}_2 = \text{H}$ ) [76]. Pathway A sees deprotonation of the amine before the bromide dissociates from the complex, leaving the negatively charged complex **10** after deprotonation. This supports the crystal structure obtained with the S-Phos ligand, which has both the bromide present and the amine *trans* to the phosphine ligand [76]. However, an alternative pathway, where bromide is lost before/during coordination of morpholine (route B), can be envisaged as well. Pathway B loses the bromide ligand first, forming a positively charged intermediate **11**, before the base  ${}^t\text{BuO}^-$  **3** deprotonates the amine. Scheme 3 illustrates both routes; charged species exist in both cases and a continuum dielectric solvation model for toluene was applied to these complexes (see Section 2).

Amine coordination gives rise to several possible isomers of **9**, **10**, **11** and **12**. The ordering of energies for these isomers follows expected *trans* influences and this has been discussed in detail in the Supporting Information; here we show the most feasible route where the ligand remains *trans* to the amine group. From **7**, where  $\text{P}^t\text{Bu}_3$  is *trans* to Br in the favoured isomer, this could have arisen by isomerisation prior to amine coordination to create the necessary vacant site *trans* to the ligand (although we have been unable to find this isomer), or by the amine coordinating between the bromide and phenyl ligands, pushing the complex into a square-planar geometry from the T-shaped arrangement of **7**. As detailed in Scheme 3, route A, the amine is then deprotonated by a base, modelled here as  ${}^t\text{BuO}^-$ . Bromide loss can occur before or after the deprotonation, with the former implicit in route B (Scheme 3).

The calculated energies (Table 2) favour pathway A, which is also in agreement with the observed crystal structure geometry for the S-Phos ligand [76]. The lower relative energies of intermediates **9** and **10** in comparison to intermediate **11** show the most likely route after oxidative addition of the phenylbromide to the complex is amine coordination to give **9**, deprotonation of the coordinated amine, giving **10**, and finally dissociation of the bromide ligand. This produces complex **12** which is the precursor to the two possible elimination routes of this catalytic cycle (discussed in Section 3.3), with a preference for the  $\text{P}^t\text{Bu}_3$  ligand **I** to be *trans* to the amido group (see Supporting Information for a more detailed discussion of isomers). This agrees with Cundari and Deng's results [45], who suggested a two-step process of deprotonation (**7**–**9**) and bromide loss (**10**–**12**). While they found the bromide loss step to be endergonic in the gas phase, both steps became exergonic when they considered  $\text{PMe}_3$  as the ligand and included solvation effects. In this context it is perhaps also worth noting recent work by Lledós and co-workers, where they analysed how amide ligands stabilise low-coordinate complexes such as **12** [78].

In summary, the calculations suggest that amine coordination and deprotonation are facile and thus unlikely to be rate-limiting, in line with the experimental observation that reaction rates are independent of base concentration [17].



**Scheme 4.** Elimination pathways from complex **12**.

### 3.3. Competing elimination pathways

From the amido complex **12**, the catalytic cycle (Scheme 2) completes with reductive elimination of the desired arylamine **14** and regeneration of the low-coordinate Pd(0) complex **1**. However, with suitable amines a  $\beta$ -hydride elimination could occur instead, forming imine **16** and then generating an aryl species, benzene **18** in the cycle studied here. These pathways are detailed in Scheme 4. While the  $\beta$ -hydride elimination pathway requires a vacant coordination site on the metal complex to accommodate the hydride, reductive elimination could occur from both three- and four-coordinate palladium complexes. However, Hartwig observed that elimination is usually faster for three-coordinate compounds [29], in line with the experimentally observed utility of complexes with bulky ligands which are more likely to be monoligated.

The desirable reductive elimination step can be achieved by appropriate choice of ligand and in this area, work by Hartwig and co-workers [2,16,28–30,79] has contributed substantially to the development of ligand design criteria. In brief, sterically hindered ligands support fast reductive elimination, whereas electron-rich ligands slow the elimination step down, as the reduction of an electron-rich metal centre becomes more difficult [30]. The  $P^tBu_3$  ligand **I** seems to represent an appropriate compromise, overcoming the disadvantage afforded by its electron-rich character with extreme steric bulk. In addition, a number of computational studies have sought to explore ligand effects on elimination steps further [9,26,31,45–48,80]. While the relative importance of steric and electronic contributions varies according to the system studied [30,31,47,80], synthetically useful ligands (Fig. 1) are often either chelating (**V–VII**), preventing the generation of a vacant site for  $\beta$ -hydride elimination, or they are monodentate but sterically demanding (**I–IV**, **VIII**), again favouring a low-coordinate route and accelerating the reductive elimination pathway.

The lowest energy isomer of intermediate **12** is T-shaped and has the deprotonated amine *trans* to the  $P^tBu_3$  ligand; this can undergo direct reductive elimination with a barrier of 10.9 kcal mol<sup>-1</sup> (Table 3; other isomers have been discussed in the Supporting Information). From **12** the coordination number decreases from three to two to form a linear adduct with the amine product, complex **13**, which lies 22.8 kcal mol<sup>-1</sup> lower in energy than **12**.  $\beta$ -Hydride elimination can also occur from the same isomer of **12**, proceeding via a barrier of 22.7 kcal mol<sup>-1</sup>. However, the reaction product is higher in energy by 5.8 kcal mol<sup>-1</sup>, as the morpholine ring makes formation of the imine unfavourable. For the bulky  $P^tBu_3$  ligand **I**, the reductive elimination pathway is thus substantially favoured over the competing  $\beta$ -hydride elimination (Table 3).

We have also explored the balance of elimination energies with  $PMe_3$  and  $PPh_3$  ligands, assuming that they follow the same dissociative mechanism as calculated for  $P^tBu_3$ , to highlight ligand effects on the transition state energies. For  $PMe_3$ , the reductive elimination step proceeds via a barrier of 12.5 kcal mol<sup>-1</sup> and the

**Table 3**

Energies for elimination steps ( $\Delta E = \Delta E_{B3LYP/BS2} + \Delta ZPE_{B3LYP/BS1}$ , see Scheme 4 for complex numbering).

Intermediate		$\Delta E$ (kcal mol <sup>-1</sup> )
$[Pd^{II}(P^tBu_3)(Ph)(NC_4H_8O)]$	<b>12</b>	0.00
<i>Reductive elimination</i>		
Transition state		10.94
$[Pd^0(P^tBu_3)(Ph)(NC_4H_8O)]$	<b>13</b>	-22.78
$[Pd^0(P^tBu_3)] + \mathbf{14}$	<b>1</b>	-9.91
<i><math>\beta</math>-Hydride elimination</i>		
Transition state		22.66
$[Pd^{II}(P^tBu_3)(Ph)(H)(NC_4H_7O)]$	<b>15</b>	5.79
$[Pd^{II}(P^tBu_3)(Ph)(H)] + \mathbf{16}$	<b>17</b>	25.26 (6.47) <sup>a</sup>
$[Pd^0(P^tBu_3)] + \mathbf{18}$	<b>1</b>	-2.99

<sup>a</sup> Energy of lowest isomer, Ph *trans* to L, in parentheses, see Supporting Information for further discussion.

barrier to  $\beta$ -hydride elimination amounts to 16.2 kcal mol<sup>-1</sup>, supporting the observation that sterically demanding ligands such as  $P^tBu_3$  (**I**) essentially prevent the  $\beta$ -hydride elimination step through increased steric hindrance, whereas this side reaction remains energetically feasible for smaller alkylphosphines. In addition, reductive elimination is comparatively more difficult for the smaller  $PMe_3$  ligand, suggesting that compared to  $P^tBu_3$ , a good donor ligand (thus worse for reductive elimination) with less steric hindrance is indeed giving rise to a higher barrier for this step. Similarly, with a  $PPh_3$  ligand, barriers to reductive elimination and  $\beta$ -hydride elimination are calculated as 11.1 and 15.7 kcal mol<sup>-1</sup>, respectively, and side-products arising from the hydride elimination pathway may thus be observed in this case. While bisligation or some other form of associative mechanism becomes more likely for these smaller ligands and an exploration of these alternatives lies outside the scope of this work, it is nevertheless illustrative to compare ligand effects on the elimination barriers. It is also worth noting that ZPE corrections have a substantial effect on the balance of elimination barriers and are thus crucial for reproducing the correct trend when considering smaller ligands, where the  $\beta$ -hydride elimination pathway is more competitive.

## 4. Conclusions

We have explored the catalytic cycle for the amination of phenyl bromide with morpholine, catalysed by a  $Pd(P^tBu_3)$  complex, using density functional theory calculations. We have mapped the likely cycle and explored the stability of unreactive dimer intermediates, as well as assessing the competing elimination pathways quantitatively. In contrast to computational studies of model systems, consideration of realistic catalysts and substrates provides a valuable opportunity for the validation of both our computational approach and of general criteria used in the design of novel ligand types. Calculated barriers also allow us to quantify the differences between competing pathways, and to assess the structural

and electronic features leading to such observed preferences. Here, we have been able to highlight the role of the steric bulk of the  $P^tBu_3$  ligand in favouring a low-coordinate reaction pathway, preventing dimerisation and disfavoured  $\beta$ -hydride elimination. This work forms part of an ongoing large-scale exploration of ligand effects in transition metal complexes [51], and we are currently expanding our mechanistic studies to a more diverse ligand set, as well as considering potentially competing bisligated pathways and exploring dispersion effects on the calculated barriers.

## Acknowledgements

We are grateful for the following support: the EPSRC for the award of Advanced Research Fellowships (EP/E059376/1 and GR/S51059/01) to NF and JNH, the EPSRC and the Cambridge Crystallographic Data for PhD funding (CLM), and funding from the Department of Education and Universities DEIU of the Autonomous Government of Catalonia (MB). We would also like to thank our colleagues Prof. Guy Lloyd-Jones, Dr. Jesús Jover Modrego and Dr. Gareth Owen-Smith at the University of Bristol and Dr. Paul Murray, Dr. Bob Osborne, Dr. Mark Purdie and Dr. Dave Hose at AstraZeneca Process Research and Design for many helpful discussions of cross-coupling reactions.

## Appendix A. Supplementary data

Supplementary data associated with this article can be found, in the online version, at doi:10.1016/j.molcata.2010.02.030.

## References

- [1] M.N. Birkholz, Z. Freixa, P. van Leeuwen, *Chem. Soc. Rev.* 38 (2009) 1099–1118; S.L. Buchwald, *Acc. Chem. Res.* 41 (2008) 1439–1564, and references cited.
- [2] J.F. Hartwig, *Nature* 455 (2008) 314–322.
- [3] D.S. Surry, S.L. Buchwald, *Angew. Chem. Int. Ed.* 47 (2008) 6338–6361.
- [4] E.A.B. Kantchev, C.J. O'Brien, M.G. Organ, *Angew. Chem. Int. Ed.* 46 (2007) 2768–2813; V. Farina, *Adv. Synth. Catal.* 346 (2004) 1553–1582.
- [5] S.L. Buchwald, C. Mauger, G. Mignani, U. Scholz, *Adv. Synth. Catal.* 348 (2006) 23–39; J.S. Carey, D. Laffan, C. Thomson, M.T. Williams, *Org. Biomol. Chem.* 4 (2006) 2337–2347.
- [6] U. Christmann, R. Vilar, *Angew. Chem. Int. Ed.* 44 (2005) 366–374, and references cited.
- [7] J.-P. Corbet, G. Mignani, *Chem. Rev.* 106 (2006) 2651–2710, and references cited.
- [8] B. Schlummer, U. Scholz, *Adv. Synth. Catal.* 346 (2004) 1599–1626.
- [9] J.D. Hicks, A.M. Hyde, A.M. Cuezva, S.L. Buchwald, *J. Am. Chem. Soc.* 131 (2009) 16720–16734.
- [10] G.C. Fu, *Acc. Chem. Res.* 41 (2008) 1555–1564.
- [11] J.F. Hartwig, *Acc. Chem. Res.* 41 (2008) 1534–1544, and references cited.
- [12] Q. Shen, T. Ogata, J.F. Hartwig, *J. Am. Chem. Soc.* 130 (2008) 6586–6596.
- [13] M. Ahlquist, P.-O. Norrby, *Organometallics* 26 (2007) 550–553.
- [14] T.E. Barder, S.D. Walker, J.R. Martinelli, S.L. Buchwald, *J. Am. Chem. Soc.* 127 (2005) 4685–4696; A.F. Littke, C.Y. Dai, G.C. Fu, *J. Am. Chem. Soc.* 122 (2000) 4020–4028; A.F. Littke, G.C. Fu, *Angew. Chem. Int. Ed.* 41 (2002) 4176–4211.
- [15] F. Barrios-Landeros, J.F. Hartwig, *J. Am. Chem. Soc.* 127 (2005) 6944–6945.
- [16] J.F. Hartwig, M. Kawatsura, S.I. Hauck, K.H. Shaughnessy, L.M. Alcazar-Roman, *J. Org. Chem.* 64 (1999) 5575–5580.
- [17] S. Shekhar, J.F. Hartwig, *Organometallics* 26 (2007) 340–351.
- [18] J.P. Stambuli, M. Buehl, J.F. Hartwig, *J. Am. Chem. Soc.* 124 (2002) 9346–9347.
- [19] S. Urganakar, M. Nagarajan, J.G. Verkade, *J. Org. Chem.* 68 (2003) 452–459.
- [20] A.G. Sergeev, A. Zapf, A. Spannenberg, M. Beller, *Organometallics* 27 (2008) 297–300.
- [21] A. Ehrentraut, A. Zapf, M. Beller, *A New Improved Catalyst for the Palladium-Catalyzed Amination of Aryl Chlorides*, Lyon, France, 2001, pp. 515–523.
- [22] S. Shekhar, P. Ryberg, J.F. Hartwig, J.S. Mathew, D.G. Blackmond, E.R. Strieter, S.L. Buchwald, *J. Am. Chem. Soc.* 128 (2006) 3584–3591, and references cited.
- [23] M.S. Driver, J.F. Hartwig, *J. Am. Chem. Soc.* 118 (1996) 7217–7218.
- [24] N. Marion, S.P. Nolan, *Acc. Chem. Res.* 41 (2008) 1440–1449, and references cited.
- [25] T.E. Barder, M.R. Biscoe, S.L. Buchwald, *Organometallics* 26 (2007) 2183–2192.
- [26] T.E. Barder, S.L. Buchwald, *J. Am. Chem. Soc.* 129 (2007) 12003–12010.
- [27] J.P. Stambuli, C.D. Incarvito, M. Buehl, J.F. Hartwig, *J. Am. Chem. Soc.* 126 (2004) 1184–1194.
- [28] J.F. Hartwig, S. Richards, D. Baranano, F. Paul, *J. Am. Chem. Soc.* 118 (1996) 3626–3633; M. Yamashita, J.F. Hartwig, *J. Am. Chem. Soc.* 126 (2004) 5344–5345.
- [29] J.F. Hartwig, *Pure Appl. Chem.* 71 (1999) 1417–1423.
- [30] J.F. Hartwig, *Inorg. Chem.* 46 (2007) 1936–1947.
- [31] V.P. Ananikov, D.G. Musaev, K. Morokuma, *Eur. J. Inorg. Chem.* (2007) 5390–5399.
- [32] J.P. Stambuli, S.R. Stauffer, K.H. Shaughnessy, J.F. Hartwig, *J. Am. Chem. Soc.* 123 (2001) 2677–2678; S.R. Stauffer, J.F. Hartwig, *J. Am. Chem. Soc.* 125 (2003) 6977–6985; P.J. Fagan, E. Hauptmann, R. Shapiro, A. Casalnuovo, *J. Am. Chem. Soc.* 122 (2000) 5043–5051.
- [33] C. Amatore, A. Jutand, *Acc. Chem. Res.* 33 (2000) 314–321, and references cited; M.R. an der Heiden, H. Plenio, S. Immel, E. Burello, G. Rothenberg, H.C.J. Hoefloot, *Chem. Eur. J.* 14 (2008) 2857–2866; A.C. Ferretti, J.S. Mathew, I. Ashworth, M. Purdy, C. Brennan, D.G. Blackmond, *Adv. Synth. Catal.* 350 (2008) 1007–1012; R.A. Gossage, H.A. Jenkins, N.D. Jones, R.C. Jones, B.F. Yates, *Dalton Trans.* (2008) 3115–3122; R.B. Jordan, *Organometallics* 26 (2007) 4763–4770; A. Jutand, *Chem. Rev.* 108 (2008) 2300–2347; E.R. Strieter, S.L. Buchwald, *Angew. Chem. Int. Ed.* 45 (2006) 925–928.
- [34] F. Barrios-Landeros, B.P. Carrow, J.F. Hartwig, *J. Am. Chem. Soc.* 131 (2009) 8141–8154.
- [35] F. Barrios-Landeros, B.P. Carrow, J.F. Hartwig, *J. Am. Chem. Soc.* 130 (2008) 5842–5843.
- [36] E.A. Mitchell, P.G. Jessop, M.C. Baird, *Organometallics* 28 (2009) 6732–6738.
- [37] A.A.C. Braga, G. Ujaque, F. Maseras, *Organometallics* 25 (2006) 3647–3658.
- [38] L.J. Goossen, D. Koley, H.L. Hermann, W. Thiel, *Organometallics* 25 (2006) 54–67, and references cited.
- [39] K. Albert, P. Gisdakis, N. Roesch, *Organometallics* 17 (1998) 1608–1616; U. Christmann, D.A. Pantazis, J. Benet-Buchhols, J.E. McGrady, F. Maseras, R. Vilar, *J. Am. Chem. Soc.* 128 (2006) 6376–6390; S.T. Henriksen, P.-O. Norrby, P. Kaukoranta, P.G. Andersson, *J. Am. Chem. Soc.* 130 (2008) 10414–10421; R.B. DeVasher, J.M. Spruell, D.A. Dixon, G.A. Broker, S.T. Griffin, R.D. Rogers, K.H. Shaughnessy, *Organometallics* 24 (2005) 962–971.
- [40] S. Kozuch, C. Amatore, A. Jutand, S. Shaik, *Organometallics* 24 (2005) 2319–2330, and references cited.
- [41] S. Kozuch, S. Shaik, *J. Am. Chem. Soc.* 128 (2006) 3355–3365, and references cited.
- [42] Z. Li, Y. Fu, Q.-X. Guo, L. Liu, *Organometallics* 27 (2008) 4043–4049.
- [43] R. Fazaeli, A. Ariaifard, S. Jamshidi, E.S. Tabatabaie, K.A. Pishro, *J. Organomet. Chem.* 692 (2007) 3984–3993.
- [44] J.C. Green, B.J. Herbert, R. Lonsdale, *J. Organomet. Chem.* 690 (2005) 6054–6067.
- [45] T.R. Cundari, J. Deng, *J. Phys. Org. Chem.* 18 (2005) 417–425.
- [46] A. Ariaifard, B.F. Yates, *J. Am. Chem. Soc.* 131 (2009) 13981–13991.
- [47] A. Ariaifard, B.F. Yates, *J. Organomet. Chem.* 694 (2009) 1075–2084.
- [48] M. Perez-Rodriguez, A.A.C. Braga, M. Garcia-Melchor, M.H. Perez-Temprano, J.A. Casares, G. Ujaque, A.R. de Lera, R. Alvarez, F. Maseras, P. Espinet, *J. Am. Chem. Soc.* 131 (2009) 3650–3657.
- [49] C. Bo, F. Maseras, *Dalton Trans.* (2008) 2911–2919.
- [50] T.R. Cundari, J. Deng, Y. Zhao, *J. Mol. Struct. Theochem.* 632 (2003) 121–129.
- [51] N. Fey, A. Tsipis, S.E. Harris, J.N. Harvey, A.G. Orpen, R.A. Mansson, *Chem. Eur. J.* 12 (2006) 291–302; R.A. Mansson, A.H. Welsh, N. Fey, A.G. Orpen, *J. Chem. Inform. Model.* 46 (2006) 2591–2600; N. Fey, J.N. Harvey, G.C. Lloyd-Jones, P. Murray, A.G. Orpen, R. Osborne, M. Purdie, *Organometallics* 27 (2008) 1372–1383; N. Fey, M.F. Haddow, J.N. Harvey, C.L. McMullin, A.G. Orpen, *Dalton Trans.* (2009) 8183–8196.
- [52] L.L. Hill, L.R. Moore, R. Huang, R. Craciun, A.J. Vincent, D.A. Dixon, J. Chou, C.J. Woltermann, K.H. Shaughnessy, *J. Org. Chem.* 71 (2006) 5117–5125; J.P. Wolfe, H. Tomori, J.P. Sadighi, J. Yin, S.L. Buchwald, *J. Org. Chem.* 65 (2000) 1158–1174.
- [53] A.D. Becke, *Phys. Rev. A* 38 (1988) 3098–3100; J.C. Slater, *Quantum Theory of Molecules and Solids*, Vol. 4: The Self-Consistent Field for Molecules and Solids, McGraw-Hill, New York, 1974; S.H. Vosko, L. Wilk, M. Nusair, *Can. J. Phys.* 58 (1980) 1200–1211.
- [54] A.D. Becke, *J. Chem. Phys.* 98 (1993) 5648–5652.
- [55] Jaguar 6.0, Schrödinger LLC, New York, NY, 2005.
- [56] J.P. Perdew, *Phys. Rev. B* 33 (1986) 8822–8824; J.P. Perdew, *Phys. Rev. B* 34 (1986) 7406.
- [57] M.J. Frisch, M. Head-Gordon, J.A. Pople, *Chem. Phys. Lett.* 166 (1990) 275; M.J. Frisch, M. Head-Gordon, J.A. Pople, *Chem. Phys. Lett.* 166 (1990) 281; M. Head-Gordon, T. Head-Gordon, *Chem. Phys. Lett.* 220 (1994) 122; M. Head-Gordon, J.A. Pople, M.J. Frisch, *Chem. Phys. Lett.* 153 (1988) 503; C. Møller, M.S. Plesset, *Phys. Rev.* 46 (1934) 618; S. Saebø, J. Almlof, *Chem. Phys. Lett.* 154 (1989) 83.
- [58] J. Cizek, *Adv. Chem. Phys.* 14 (1969) 35; J.A. Pople, M. Head-Gordon, K. Raghavachari, *J. Chem. Phys.* 87 (1987) 5968; G.D. Purvis, R.J. Bartlett, *J. Chem. Phys.* 76 (1982) 1910; G.E. Scuseria, C.L. Janssen, H.F. Schaeffer III, *J. Chem. Phys.* 89 (1988) 7382; G.E. Scuseria, H.F. Schaeffer III, *J. Chem. Phys.* 90 (1989) 3700.
- [59] M.J. Frisch, G.W. Trucks, H.B. Schlegel, G.E. Scuseria, M.A. Robb, J.R. Cheeseman, J. Montgomery, J.A., T. Vreven, K.N. Kudin, J.C. Burant, J.M. Millam, S.S.

- Iyengar, J. Tomasi, V. Barone, B. Mennucci, M. Cossi, G. Scalmani, N. Rega, G.A. Petersson, H. Nakatsuji, M. Hada, M. Ehara, K. Toyota, R. Fukuda, J. Hasegawa, M. Ishida, T. Nakajima, Y. Honda, O. Kitao, H. Nakai, M. Klene, X. Li, J.E. Knox, H.P. Hratchian, J.B. Cross, V. Bakken, C. Adamo, J. Jaramillo, R. Gomperts, R.E. Stratmann, O. Yazyev, A.J. Austin, R. Cammi, C. Pomelli, J.W. Ochterski, P.Y. Ayala, K. Morokuma, G.A. Voth, P. Salvador, J.J. Dannenberg, V.G. Zakrzewski, S. Dapprich, A.D. Daniels, M.C. Strain, O. Farkas, D.K. Malick, A.D. Rabuck, K. Raghavachari, J.B. Foresman, J.V. Ortiz, Q. Cui, A.G. Baboul, S. Clifford, J. Cioslowski, B.B. Stefanov, G. Liu, A. Liashenko, P. Piskorz, I. Komaromi, R.L. Martin, D.J. Fox, T. Keith, M.A. Al-Laham, C.Y. Peng, A. Nanayakkara, M. Challacombe, P.M.W. Gill, B. Johnson, W. Chen, M.W. Wong, C. Gonzalez, J.A. Pople, Gaussian 03, Revision C.02, Wallingford, CT, 2004.
- [60] D. Andrae, U. Haeussermann, M. Dolg, H. Stoll, H. Preuss, *Theor. Chim. Acta* 77 (1990) 123–141.
- [61] H.-J. Werner, P.J. Knowles, R. Lindh, F.R. Manby, M. Schuetz, P. Celani, T. Korona, A. Mitrushenkov, G. Rauhut, T.B. Adler, R.D. Amos, A. Bernhardsson, A. Berning, D.L. Cooper, M.J.O. Deegan, A.J. Dobbyn, F. Eckert, E. Goll, C. Hampel, G. Hetzer, T. Hrenar, G. Knizia, C. Koeppl, Y. Liu, A.W. Lloyd, R.A. Mata, A.J. May, S.J. McNicholas, W. Meyer, M.E. Mura, A. Nicklass, P. Palmieri, K. Pflueger, R. Pitzer, M. Reiher, U. Schumann, H. Stoll, A.J. Stone, R. Tarroni, T. Thorsteinsson, M. Wang, A. Wolf, MOLPRO, Version 2002.6, a Package of Ab Initio Programs, Cardiff, UK, 2004.
- [62] P.J. Knowles, C. Hampel, H.-J. Werner, *J. Chem. Phys.* 99 (1993) 5219; P.J. Knowles, C. Hampel, H.-J. Werner, *J. Chem. Phys.* 112 (2000) 3106; J.D. Watts, J. Gauss, R.J. Bartlett, *J. Chem. Phys.* 98 (1993) 8718.
- [63] J.M.L. Martin, A. Sundermann, *J. Chem. Phys.* 114 (2001) 3408–3420.
- [64] D.E. Woon, T.H. Dunning, *J. Chem. Phys.* 98 (1993) 1358–1371; D.E. Woon, T.H. Dunning, *J. Chem. Phys.* 103 (1995) 4572–4585.
- [65] S. Grimme, *J. Chem. Phys.* 118 (2003) 9095–9102.
- [66] Y. Minenkov, G. Occhipinti, V.R. Jensen, *J. Phys. Chem. A* 113 (2009) 11833–11844.
- [67] B. Marten, K. Kim, C. Cortis, R.A. Friesner, R.B. Murphy, M.N. Ringnalda, D. Sitkoff, B. Honig, *J. Phys. Chem.* 100 (1996) 11775; D.J. Tannor, B. Marten, R. Murphy, R.A. Friesner, D. Sitkoff, A. Nicholls, M. Ringnalda, W.A. Goddard III, B. Honig, *J. Am. Chem. Soc.* 116 (1994) 11875.
- [68] H.M. Senn, T. Ziegler, *Organometallics* 23 (2004) 2980–2988.
- [69] M. Ahlquist, P. Fristrup, D. Tanner, P.-O. Norrby, *Organometallics* 25 (2006) 2066–2073.
- [70] S. Moncho, G. Ujaque, A. Lledós, P. Espinet, *Chem. Eur. J.* 17 (2008) 8986–8994.
- [71] S. Kozuch, S. Shaik, A. Jutand, C. Amatore, *Chem. Eur. J.* 10 (2004) 3072–3080.
- [72] J.N. Harvey, J. Jover, G.C. Lloyd-Jones, J.D. Moseley, P. Murray, J.S. Renny, *Angew. Chem. Int. Ed.* 48 (2009) 7612–7615; J. Jover, N. Fey, M. Purdie, G.C. Lloyd-Jones, J.N. Harvey, *J. Mol. Catal. A* 324 (2010) 39–47.
- [73] J.P. Stambuli, R. Kuwano, J.F. Hartwig, *Angew. Chem. Int. Ed.* 41 (2002) 4746–4748, and references cited.
- [74] E.A. Mitchell, M.C. Baird, *Organometallics* 26 (2007) 5230–5238.
- [75] L.J. Goossen, D. Koley, H.L. Hermann, W. Thiel, *Chem. Commun.* (2004) 2141–2143.
- [76] M.R. Biscoe, T.E. Barder, S.L. Buchwald, *Angew. Chem. Int. Ed.* 46 (2007) 7232–7235.
- [77] F. Paul, J. Patt, J.F. Hartwig, *Organometallics* 14 (1995) 3030–3039.
- [78] S. Moncho, G. Ujaque, P. Espinet, F. Maseras, A. Lledós, *Theor. Chem. Acc.* 123 (2009) 75–84.
- [79] J.F. Hartwig, *Acc. Chem. Res.* 31 (1998) 852–860; M. Yamashita, J.V.C. Vicario, J.F. Hartwig, *J. Am. Chem. Soc.* 125 (2003) 16347–16360; D.A. Culkin, J.F. Hartwig, *Organometallics* 23 (2004) 3398–3416; S. Shekhar, J.F. Hartwig, *J. Am. Chem. Soc.* 126 (2004) 13016–13027.
- [80] E. Zuidema, P.W.N.M. van Leeuwen, C. Bo, *Organometallics* 24 (2005) 3703–3710.